

Template-Free Synthesis of Single-/Double-Walled TiO₂ Nanovesicles: Potential Photocatalysts for Engineering Application

Gongde Chen, He Cheng, Weixin Zhang, Zeheng Yang, Maoqin Qiu, Xiao Zhu, and Min Chen

Dept. of Chemical Engineering and Technology, School of Chemistry and Chemical Engineering, Anhui Key Laboratory of Controllable Chemical Reaction & Material Chemical Engineering, Hefei University of Technology, Hefei, Anhui 230009, P.R. China

DOI 10.1002/aic.14774

Published online March 11, 2015 in Wiley Online Library (wileyonlinelibrary.com)

Significance Single- and double-walled anatase TiO₂ nanovesicles have been, respectively, prepared by a template-free hydrothermal treatment of Ti(SO₄)₂ with H₂O₂ and urea. Photocatalytic degradation of Rhodamine B indicates that double-walled TiO₂ nanovesicles have an initial lower but a final higher photocatalytic efficiency than single-walled ones. All nanovesicles have significantly lower performance than commercially available P25 TiO₂. The enhanced capacity for UV light absorption and ·OH radicals production, large specific surface area, and unique hierarchical hollow architectures contribute to the enhanced photocatalytic activity and improved feasibility of anatase TiO₂ nanovesicles for engineering applications. © 2015 American Institute of Chemical Engineers *AIChE J.* 61: 1478–1482, 2015

Keywords: TiO₂, double walls, hollow nanostructures, Rhodamine B, photocatalysis

Multiwall/shell hollow nanostructures have spurred more and more interests owing to their superior properties with the advancement of nanoscience.^{1–3} Multishelled TiO₂ hollow spheres present superior photocatalytic activity to sphere-in-sphere and nanoparticle samples because of the enhancement of light absorbance resulted from multiple reflections of UV light within the interior cavity.² However, the vast majority of existing studies focus on design and fabrication of simple TiO₂ hollow nanostructures with single wall/shell.^{4,5} There are only a few reports on the preparation of multishelled TiO₂ hollow nanostructures based on template method.^{2,6–8} For instance, Yao et al.² prepared multishelled TiO₂ hollow spheres by immersing porous polystyrene-divinyl-benzene spheres into the titania sol and subsequent postcalcination. Wang et al.⁸ prepared shell-in-shell TiO₂ hollow spheres through hydrothermal treatment of TiF₄ and sucrose followed by removing carbonaceous cores and shells through calcination.

Although template method is the general way for preparing TiO₂ hollow nanostructures, it is subject to tedious procedures in surface modification, template removing, and postheat treatment for crystallization which is likely to con-

sume more energy, reduce the specific surface area and even lead to the collapse of the hollow structures. Recent studies show that solution-phase chemical synthesis under hydrothermal conditions is not only effective for architecture control but also has great potential for large-scale production in terms of operation, cost, and throughput.^{9,10} However, till now, it is still a challenge to prepare multiwall/shell TiO₂ hollow nanostructures by this method.

In this letter, a one-pot template-free method is presented for the first time to synthesize single- and double-walled anatase TiO₂ nanovesicles by hydrothermal treatment of Ti(SO₄)₂ with the assistance of H₂O₂ and urea. It is interesting to demonstrate that double-walled anatase TiO₂ nanovesicles have different photocatalytic activity from single-walled anatase TiO₂ nanovesicles at different stages of the degradation process. Anatase TiO₂ nanovesicles with unique hierarchical hollow structures not only enhance light harvesting capacity and offer large surface area for photocatalytic reaction but also are expected to overcome some practical problems encountered by particulate TiO₂ catalysts such as strong tendency of agglomeration and difficult postseparation and recycling.

Experimental details for the sample synthesis and characterization were described in Supplementary Material. XRD patterns of the products obtained at 2 and 16 h are shown in Supporting Information Figure S1a. All of the observed diffraction peaks can be well indexed to tetragonal anatase TiO₂ (JCPDS No. 21–1272). The sharper diffraction peaks

Additional Supporting Information may be found in the online version of this article.

Correspondence concerning this article should be addressed to W. Zhang at wxzhang@hfut.edu.cn.

© 2015 American Institute of Chemical Engineers

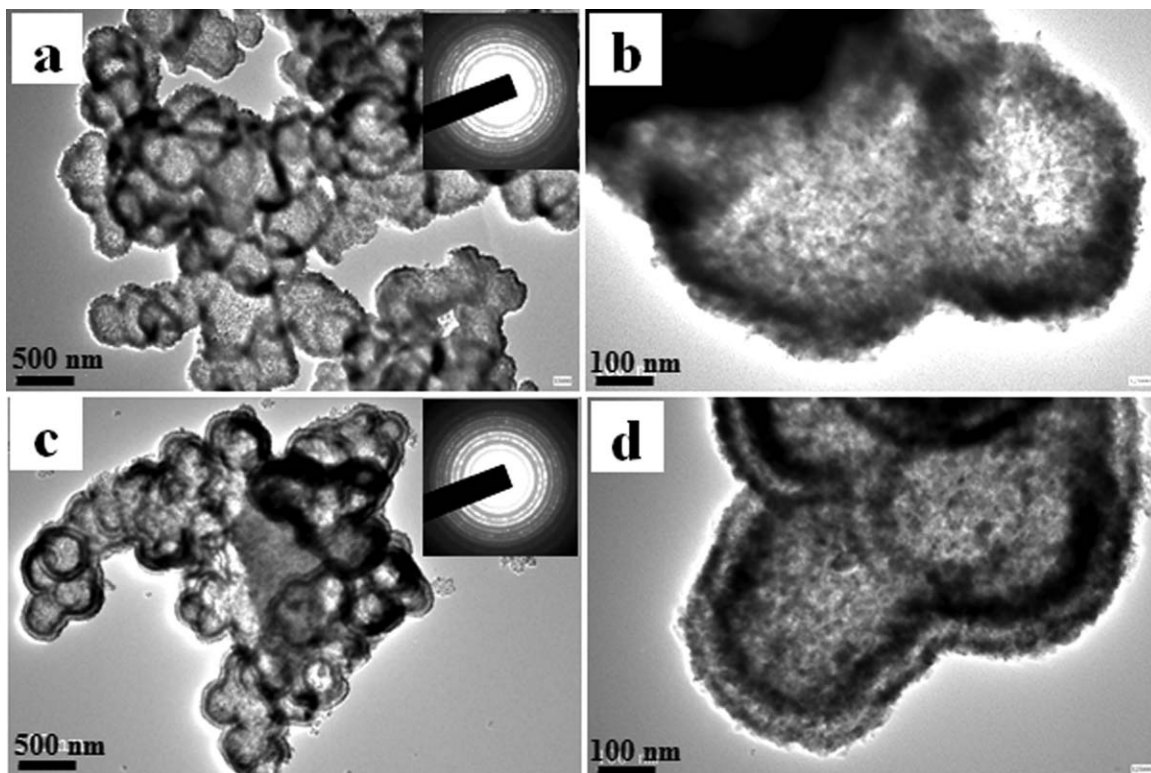


Figure 1. TEM images of anatase TiO_2 samples prepared by a hydrothermal treatment of $\text{Ti}(\text{SO}_4)_2$ with the assistance of H_2O_2 and urea for (a, b) 2 h and (c, d) 16 h. (The insets: SAED patterns of the samples).

with the increasing reaction time reveal the improvement of the crystallinity with bigger crystallite size. Nitrogen sorption experimental results in Supporting Information Figure S1b show that both of the samples have a type-IV isotherm with a hysteresis loop, indicating their mesoporous structure.¹¹ The BET surface area of the samples obtained at 2 and 16 h is 170.1 and 106.2 m^2/g with the average pore diameter of 3.76 and 7.59 nm, respectively, and the former displays a narrower pore size distribution than the latter.

TEM images in Figures 1a, b show that anatase TiO_2 sample obtained at 2 h displays single-walled vesicle-like nanostructures with sizes ranging from 400 to 500 nm, which are interconnected with each other to form larger aggregates at micrometer scale and are consistent with their FESEM observation (see Supporting Information Figures S2a, b). Actually, the nanovesicle wall with thickness of about 100 nm is composed of small nanoparticles with sizes of 15 nm. When the reaction time prolongs to 16 h, double-walled TiO_2 vesicle-like hollow nanostructures with sizes ranging from 400 to 500 nm can be clearly observed in Figures 1c, d, which is also in agreement with their FESEM results (see Supporting Information Figures S2c, d). The inner and outer walls with a spacing of 10–20 nm have a thickness of around 30 and 50 nm, respectively. Double-walled nanovesicles are also aggregated into larger particles at micrometer scale and assembled by nanoparticles with larger sizes (around 30 nm) than single-walled nanovesicles. SAED patterns of the two TiO_2 samples shown in the inset of Figures 1a, c are both ring-like, suggesting that they are polycrystalline.

The formation process of single- and double-walled anatase TiO_2 nanovesicles is shown in Supporting Information Figure S3. Ti^{4+} ions gradually hydrolyzed in the circumstance of H_2O_2 and urea aqueous solution and small nanoparticles were initially formed at 15 min, which gradually developed into metastable $\text{H}_2\text{Ti}_5\text{O}_{11} \cdot 3\text{H}_2\text{O}$ nanosheet assemblies at 30 min (see Supporting Information Figure S4a). At 1 h, more stable anatase $\text{TiO}_2/\text{H}_2\text{Ti}_5\text{O}_{11} \cdot 3\text{H}_2\text{O}$ core-shell nanostructures were formed (see Supporting Information Figure S4b). At this stage, low crystalline nanoparticles on the surface had direct contact with the surrounding solution and were first transformed to anatase crystalline layer through dissolution-recrystallization process, which were served as the nucleation seeds for subsequent recrystallization process. Poorly crystalline nanoparticles underneath the surface were dissolved gradually and recrystallized on the surface, leading to the inward evacuation and thus the formation of a core-shell structure.¹² At 2 h, the inner cores were completely dissolved and single-walled anatase TiO_2 nanovesicles were formed (see Figures 1a, b). However, the inner and outer surfaces of the wall have higher crystallinity than wall interior due to their direct contact with the surrounding solution. From 2 to 16 h, the relatively low crystalline nanoparticles located at the wall interior were dissolved and recrystallized on the wall surface because of the ripening effect, which led to the division of the wall into discrete regions and thus the formation of double-walled anatase TiO_2 nanovesicles at 16 h (see Figures 1c, d).

To evaluate the photocatalytic performances, anatase TiO_2 nanovesicles were used as the photocatalysts to degrade

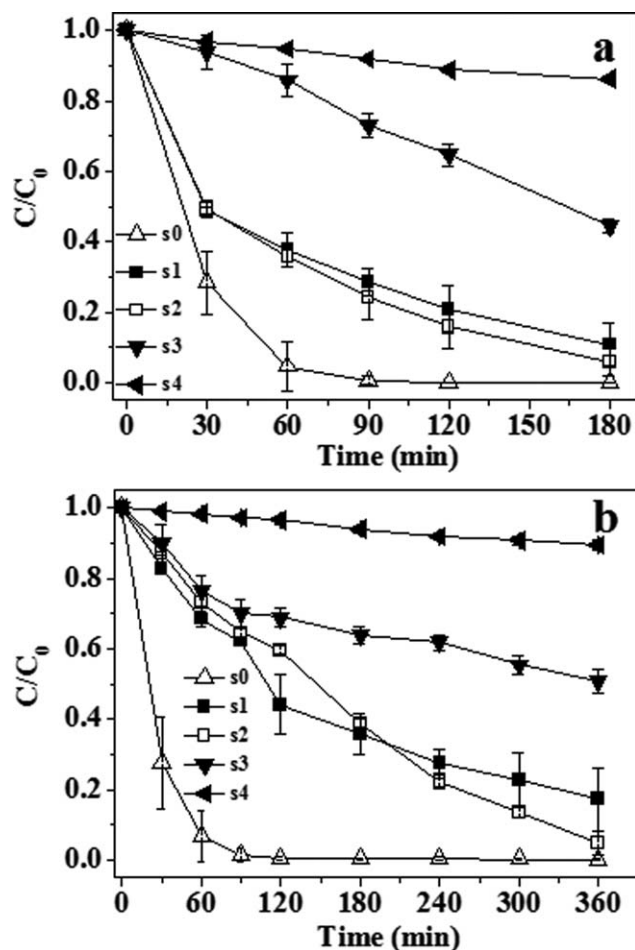


Figure 2. Photocatalytic degradation of RhB solution with an initial concentration of (a) 1×10^{-5} and (b) 2×10^{-5} mol/L under UV light irradiation in the presence of (s₀) commercially available P25 TiO₂, (s₁) single-walled anatase TiO₂ nanovesicles, (s₂) double-walled anatase TiO₂ nanovesicles, (s₃) commercial anatase TiO₂ nanoparticles, and (s₄) in the absence of any photocatalyst. Each point represents the average value of four separate experiments derived from four batches of photocatalysts, and the vertical line represents the error range.

Rhodamine B (RhB) solution in the presence of UV light. Figure 2 plots the variation of the relative concentration of RhB aqueous solution with the irradiation time. The error bars represented by vertical lines indicate that the photocatalytic performance of the photocatalysts fluctuated within certain range. As shown in Figure 2a, after 180 min of illumination, the average RhB degradation ratio over single- and double-walled anatase TiO₂ nanovesicles and commercially acquired anatase TiO₂ nanoparticles can reach 89.2, 94.2, and 55.6%, respectively. When the initial concentration of RhB aqueous solution was increased from 1×10^{-5} to 2×10^{-5} mol/L, interestingly, single-walled anatase TiO₂ nanovesicles initially present higher photocatalytic efficiency than double-walled TiO₂ nanovesicles (see Figure 2b). With further extending the reaction time, the performance of the latter surpasses that of the former. The average degradation

ratio of RhB over double-walled anatase TiO₂ nanovesicles can reach 95.0% after 360 min, which is much higher than that over single-walled anatase TiO₂ nanovesicles (82.7%) and the commercial anatase TiO₂ nanoparticles (49.3%), respectively, (see Figure 2b). A blank experiment was also conducted under UV light irradiation in the absence of any photocatalyst. The photolysis ratio of RhB with initial concentration of 1×10^{-5} and 2×10^{-5} mol/L is merely 13.7 and 10.6 %, manifesting that photocatalysts play a dominant role in the decomposition of RhB molecules.

It is interesting to find that double-walled anatase TiO₂ nanovesicles have different photocatalytic activity from single-walled anatase TiO₂ nanovesicles at different stages of the degradation reaction (see Figure 2b). Based on their adsorption curves (see Supporting Information Figure S5), more RhB molecules could be adsorbed and were finally degraded over single-walled anatase TiO₂ nanovesicles at the initial stage of the reaction because they have larger specific surface area than double-walled anatase TiO₂ nanovesicles (see Supporting Information Table 1), thus leading to their initially higher photocatalytic efficiency than that over double-walled anatase TiO₂ nanovesicles. However, double-walled anatase TiO₂ nanovesicles are able to produce more OH radicals than single-walled ones (see Supporting Information Figure S6) possibly because the former possesses higher crystallinity than the latter (see Supporting Information Figure S1a), which leads to lower recombination rate for electron-hole pairs on the former than on the latter. In addition, double-walled anatase TiO₂ nanovesicles have a lower internal diffusion resistance for RhB molecules (diameter: 1.6 nm, tending to aggregate and form dimmers with the increasing concentration)¹³ than single-walled anatase TiO₂ nanovesicles because the pore size of the former (7.59 nm) was larger than that of the latter (3.76 nm) (see Supporting Information Table 1). Thus, double-walled anatase TiO₂ nanovesicles have a final higher photocatalytic efficiency than single-walled anatase TiO₂ nanovesicles.

Single- and double-walled anatase TiO₂ nanovesicles exhibit superior photocatalytic activity to the commercial anatase TiO₂ nanoparticles. It can be rationally explained by the following aspects. First, TiO₂ nanovesicles have much larger specific surface area (see Supporting Information Table 1) and thus provide more active sites than the commercial anatase TiO₂ nanoparticles.¹⁴ Second, the diffusion reflectance UV-vis absorption spectra indicate that single- and double-walled anatase TiO₂ nanovesicles exhibit superior light absorption capacity to the commercial anatase TiO₂ nanoparticles within the wavelength range from 200 to 335 nm (see Supporting Information Figure S7) because their interior cavity and shells with accessible mesopores allow the scattering and reflecting of the light within hollow structures, extend the distance that the light travels, and enhance the light harvesting.¹⁵ In addition, single- and double-walled anatase TiO₂ nanovesicles are able to generate more OH radicals than the commercial anatase TiO₂ nanoparticles (see Supporting Information Figure S6). Thus, the as-prepared anatase TiO₂ nanovesicles offer more available photogenerated electrons and holes for the photocatalytic degradation of contaminants, leading to their enhanced photocatalytic performance in comparison with the commercial anatase TiO₂ nanoparticles.

Evonik P25 is also used as the benchmark for evaluating the prepared TiO₂ photocatalysts. RhB was nearly degraded completely over P25 at 90 min (see Figure 2: s0) under the same catalytic conditions. Although single- and double-walled anatase TiO₂ nanovesicles have a little bit lower photocatalytic efficiency than P25, their photocatalytic performances are not that comparable because they have different composition. P25, which has a particle size of around 30 nm and specific surface area of 36.4 m²/g (see Supporting Information Figure S8 and Table 1), consists of mixed phases (about 80% anatase and 20% rutile, see Supporting Information Figure S8a), whereas the as-prepared TiO₂ nanovesicles are pure anatase.

Actually, single- and double-walled anatase TiO₂ nanovesicles present some advantages over P25 not only in preparation but also in practical application. First, P25 is readily available and produced commercially at tons/h. It is prepared from titanium tetrachloride vapor in an oxyhydrogen flame hydrolysis at around 1000°C, whereas single- and double-walled anatase TiO₂ nanovesicles are synthesized via mild hydrothermal reaction at 170°C, which facilitates the operation and lowers the energy consumption for large-scale production. Meanwhile, single- and double-walled nanovesicles not only have hierarchical hollow structures assembled by small nanocrystallites, but also are interconnected to form much larger aggregates at micrometer scale. This structural characteristics make them not only inherit nanoscale properties such as large surface area and high activity but also be readily separated from solutions through initial gravity sedimentation followed by some other separation technologies. Life cycle assessment also indicates that RhB degradation ratio can still reach 81.0 and 82.8% over single- and double-walled anatase TiO₂ nanovesicles after five cycles (see Supporting Information Figure S9), indicating their good stability as photocatalysts.

In addition, the photocatalytic performance of single- and double-walled anatase TiO₂ nanovesicles can be further enhanced by improving their crystallinity and tuning their phase composition. For example, pure anatase phase can be transformed into mixing phases with certain ratio of anatase and rutile via postheat treatment. Through further optimization for process parameters, the as-prepared photocatalysts would have comparable photocatalytic performance with P25 and be more practical for large scale photocatalytic application.

In brief, single- and double-walled anatase TiO₂ nanovesicles were successfully fabricated via a simple hydrothermal treatment of Ti(SO₄)₂ with the assistance of H₂O₂ and urea. The evolution process reveals that anatase TiO₂ nanovesicles with single- and double walls are controllably transformed from H₂Ti₅O₁₁·3H₂O nanosheet assemblies using urea and H₂O₂ to tune the nucleation kinetics and dissolution-recrystallization process. Photocatalytic degradation of RhB demonstrates that double-walled anatase TiO₂ nanovesicles have an initial lower but a final higher photocatalytic efficiency than single-walled anatase TiO₂ nanovesicles at relatively higher RhB concentration. They both possess enhanced photocatalytic activity than the commercial anatase TiO₂ nanoparticles. Their unique hierarchical hollow structures

facilitate postseparation and increase their feasibility for engineering applications. This work opens a new avenue to large-scale preparation of potential TiO₂ photocatalysts and expects their wide applications in environmental remediation.

Acknowledgment

The authors are grateful for the financial support by the National Natural Science Foundation of China (NSFC Grants 20976033, 21176054, and 21271058).

Literature Cited

1. Prodan E, Radloff C, Halas NJ, Nordlander P. A hybridization model for the plasmon response of complex nanostructures. *Science*. 2003;302:419–422.
2. Zeng Y, Wang X, Wang H, Dong Y, Ma Y, Yao JN. Multi-shelled titania hollow spheres fabricated by a hard template strategy: enhanced photocatalytic activity. *Chem Commun*. 2010;46:4312–4314.
3. Zhang WX, Chen ZX, Yang ZH. An inward replacement/etching route to synthesize double-walled Cu₇S₄ nanoboxes and their enhanced performances in ammonia gas sensing. *Phys Chem Chem Phys*. 2009;11:6263–6268.
4. Lu JW, Zhang P, Li A, Su FL, Wang T, Liu Y, Gong JL. Mesoporous anatase TiO₂ nanocups with plasmonic metal decoration for highly active visible-light photocatalysis. *Chem Commun*. 2013;49:5817–5819.
5. Li J, Zeng HC. Hollowing Sn-doped TiO₂ nanospheres via ostwald ripening. *J Am Chem Soc*. 2007;129:15839–15847.
6. Ren H, Yu RB, Wang JY, Jin Q, Yang M, Mao D, Kisailus D, Zhao HJ, Wang D. Multishelled TiO₂ hollow microspheres as anodes with superior reversible capacity for lithium ion batteries. *Nano Lett* 2014;14:6679–6684.
7. Yang M, Ma J, Zhang C, Yang Z, Lu Y. General synthetic route toward functional hollow spheres with double-shelled structures. *Angew Chem Int Ed*. 2005;44:6727–6730.
8. Wu X, Lu GQ, Wang LZ. Shell-in-shell TiO₂ hollow spheres synthesized by one-pot hydrothermal method for dye-sensitized solar cell application. *Energy Environ Sci*. 2011;4:3565–3572.
9. Sun HQ, Wang SB, Ang HM, Tadé MO, Li Q. Halogen element modified titanium dioxide for visible light photocatalysis. *Chem Eng J*. 2010;162:437–447.
10. Liu Z, Sun DD, Guo P, Leckie JO. One-step fabrication and high photocatalytic activity of porous TiO₂ hollow aggregates by using a low-temperature hydrothermal method without templates. *Chem Eur J*. 2007;13:1851–1855.
11. Sing KSW, Everett DH, Haul RAW, Moscou L, Pierotti RA, Rouquerol J, Siemieniowska T. Reporting physisorption data for gas solid systems with special reference to the determination of surface-area and porosity. *Pure Appl Chem*. 1985;57:603–619.
12. Liu B, Zeng HC. Symmetric and asymmetric ostwald ripening in the fabrication of homogeneous core-shell semiconductors. *Small* 2005;1:566–571.

13. Tsunomori F, Ushiki H. Pore size effect on diffusion coefficient of rhodamine B in PNIPA gel. *Phys Lett A*. 1999;258:171–176.
14. Zhang WX, Chen GD, Yang ZH, Zeng CY. A novel approach to well-aligned TiO₂ nanotube arrays and their enhanced photocatalytic performances. *AIChE J*. 2013; 59:2134–2144.
15. Pan JH, Zhang XW, Du AJ, Sun DD, Leckie JO. Self-etching reconstruction of hierarchically mesoporous F-TiO₂ hollow microspherical photocatalyst for concurrent membrane water purifications. *J Am Chem Soc*. 2008; 130:11256–11257.

Manuscript received Jan. 3, 2015, and revision received Feb. 3, 2015,